Original Article

Mitochondrial Oxidative Stress Enhances Vasoconstriction by Altering Calcium Homeostasis in Cerebrovascular Smooth Muscle Cells under Simulated Microgravity*

LIU Zi Fan[1,&], WANG Hai Ming[1,&], JIANG Min[1], WANG Lin[1], LIN Le Jian[2], ZHAO Yun Zhang[1], SHAO Jun Jie[3], ZHOU Jing Jing[1], XIE Man Jiang[4], LI Xin[5,#], and ZHANG Ran[1,#]

1. Department of Cardiovascular Medicine, Chinese PLA General Hospital & Chinese PLA Medical School, Beijing 100853, China; 2. Department of Cardiology, The Eighth Medical Center of Chinese PLA General Hospital, Beijing 100193, China; 3. The First Clinical Medical College of Inner Mongolia Medical University, Hohhot 010059, Inner Mongolia, China; 4. Department of Aerospace Physiology, Key Laboratory of Aerospace Medicine of Ministry of Education, Fourth Military Medical University, Xi'an 710032, Shaanxi, China; 5. Division of Health services, The First Medical Center of Chinese PLA General Hospital, Beijing 100853, China

Abstract

Objective Exposure to microgravity results in postflight cardiovascular deconditioning in astronauts. Vascular oxidative stress injury and mitochondrial dysfunction have been reported during this process. To elucidate the mechanism for this condition, we investigated whether mitochondrial oxidative stress regulates calcium homeostasis and vasoconstriction in hindlimb unweighted (HU) rat cerebral arteries.

Methods Three-week HU was used to simulate microgravity in rats. The contractile responses to vasoconstrictors, mitochondrial fission/fusion, Ca^{2+} distribution, inositol 1,4,5-trisphosphate receptor (IP_3R) abundance, and the activities of voltage-gated K^+ channels (K_V) and Ca^{2+}-activated K^+ channels (BK_{Ca}) were examined in rat cerebral vascular smooth muscle cells (VSMCs).

Results An increase of cytoplasmic Ca^{2+} and a decrease of mitochondrial/sarcoplasmic reticulum (SR) Ca^{2+} were observed in HU rat cerebral VSMCs. The abundance of fusion proteins (mitofusin 1/2 [MFN1/2]) and fission proteins (dynamin-related protein 1 [DRP1] and fission-mitochondrial 1 [FIS1]) was significantly downregulated and upregulated, respectively in HU rat cerebral VSMCs. The cerebrovascular contractile responses to vasoconstrictors were enhanced in HU rats compared to control rats, and IP_3R protein/mRNA levels were significantly upregulated. The current densities and open probabilities of K_V and BK_{Ca} decreased and increased, respectively. Treatment with the mitochondrial-targeted antioxidant mitoTEMPO attenuated mitochondrial fission by upregulating MFN1/2 and downregulating DRP1/FIS1. It also decreased IP_3R expression levels and restored the activities of the K_V and BK_{Ca} channels. MitoTEMPO restored the Ca^{2+} distribution in VSMCs and attenuated the enhanced vasoconstriction in HU rat cerebral arteries.

Conclusion The present results suggest that mitochondrial oxidative stress enhances cerebral vasoconstriction by regulating calcium homeostasis during simulated microgravity.

Key words: Microgravity; Mitochondrial oxidative stress; Calcium homeostasis; Vasoconstriction

Biomed Environ Sci, 2021; 34(3): 203-212 *doi: 10.3967/bes2021.001* *ISSN: 0895-3988*

www.besjournal.com (full text) *CN: 11-2816/Q*

*This work was supported by the National Natural Science Foundation of China [81871516, 81571841] and Youth Special Project of Chinese PLA General Hospital [QNC19052].

&These authors contributed equally to this work.

#Correspondence should be addressed to LI Xin, Tel: 86-10-55499096, E-mail: lixin301@sina.cn; ZHANG Ran, Tel: 86-10-55499238, E-mail: bjzhangran@126.com

Biographical notes of the first authors: LIU Zi Fan, male, born in 1996, Bachelor, Resident Physician, majoring in space biology and cardiovascular physiology; WANG Hai Ming, male, born in 1992, Bachelor, Resident Physician, majoring in cardiology and cardiovascular physiology.

INTRODUCTION

Exposure to microgravity results in postflight cardiovascular dysfunction and orthostatic intolerance in astronauts, which poses a threat to the health of the astronauts and safety during spaceflight. Although much progress has been made in this field, the underlying mechanism remains to be established.

Studies on ground-based rodent animals have reported region-specific vascular structural and functional remodeling in hindlimb unweighting (HU) rat arteries[1-4]. Both nitric oxide (NO) and endothelin-1 in endothelial cells are modified in a simulated microgravity setting[5]. The levels of endothelial nitric oxide synthase and nitrate/nitrite content in cerebral arteries increase[6,7], which was also confirmed in human umbilical vein endothelial cells and human microvessel endothelial cells exposed to microgravity simulated by a random positioning machine and rotating wall vessel[8,9]. Calcium influx and efflux are modulated by large-conductance calcium-activated K^+ channels (BK_{Ca}) and L-type Ca^{2+} channels in HU rat cerebral vascular smooth muscle cells (VSMCs), which regulate vascular tension[10,11]. Plasma membrane calcium-regulating channels, sarco/endoplasmic reticulum Ca^{2+} ATPase, ryanodine receptors, and the inositol 1,4,5-trisphosphate receptor (IP_3R) regulate intracellular Ca^{2+} homeostasis in VSMCs[12]. The influx of extracellular Ca^{2+} and the release of Ca^{2+} from intracellular calcium stores, such as the sarcoplasmic reticulum (SR) and mitochondria regulate cellular Ca^{2+} homeostasis[13]. However, the mechanism of regulating Ca^{2+} homeostasis in VSMCs exposed to microgravity or simulated microgravity remains unclear.

Reactive oxygen species (ROS) increase cytoplasmic Ca^{2+} concentration ($[Ca^{2+}]$) by facilitating Ca^{2+} release from the endoplasmic reticulum (ER)/SR through the IP_3R[14,15]. Mitochondrial-derived ROS enhance angiotensin II-triggered vascular contraction by elevating Ca^{2+} and IP_3 levels[16]. Mitochondria regulate Ca^{2+} through fission and fusion mediated by mitofusion 1/2 (MFN1/2), dynamin-related protein 1 (DRP1), and fission protein 1 (FIS1)[17-20]. Our previous studies have detected cellular oxidative stress and mitochondrial oxidative injury in HU rat cerebral VSMCs[21-23] and inhibiting NADPH oxidase improves cerebrovascular reactivity in HU rats[7]; however, whether these factors are associated with the regulation of Ca^{2+} homeostasis and vascular remodeling is unclear. To better understand the molecular mechanisms of vascular remodeling during microgravity, the present study was designed to investigate the roles and mechanism of mitochondrial oxidative stress during Ca^{2+} homeostasis and the regulation of cerebrovascular contraction in HU rat cerebral arteries.

MATERIALS AND METHODS

The handling and treatment of animals were according to the Guiding Principles for the Care and Use of Animals in the Physiological Sciences and were approved by the Chinese guidelines for experimental animals. The care and use of experimental rats were supervised and approved by the Animal Ethical Committee of Chinese PLA General Hospital.

Ground-based Simulation of Microgravity and VSMCs Preparation

HU was used to simulate microgravity in rats as described in our previous studies[6,24]. Briefly, male Sprague-Dawley rats were randomly assigned to four groups: control (CON), HU, mitoTEMPO-treated HU (HU + MT), and mitoTEMPO-treated control (CON + MT). To simulate the cardiovascular effect of microgravity, the HU rats were maintained in about a −30° head-down tilt position and housed individually with their hindlimbs unloaded under a 12:12-h light-dark cycle at 23 ± 1 °C with food and water available *ad libitum*. The control rats were housed in identical Plexiglas cages, except that the tail suspension device was removed. HU + MT and CON + MT rats received distilled water containing mitoTEMPO (Alexis Biochemicals, San Diego, CA, USA) provided at a rate of 0.7 mg/(kg·day) by gavage. The rats in the other groups received an equal volume of vehicle (distilled water). The rats were killed by exsanguination via the abdominal aorta 3 weeks later. The cerebral arteries were rapidly removed and placed in cold Krebs buffer solution containing 118.3 mmol/L NaCl, 14.7 mmol/L KCl, 1.2 mmol/L KH_2PO_4, 1.2 mmol/L $MgSO_4·7H_2O$, 2.5 mmol/L $CaCl_2·2H_2O$, 25 mmol/L $NaHCO_3$, 11.1 mmol/L dextrose, and 0.026 mmol/L EDTA (pH 7.4). VSMCs were dissociated from cerebral arteries as described previously[11].

Western Blot

The samples were homogenized in 10 mmol/L HEPES lysis buffer (320 mmol/L sucrose, 1 mmol/L EDTA, 1 mmol/L DTT, 10 μg/mL leupeptin, and

2 μg/mL aprotinin, pH 7.40) at 0–4 °C. The homogenate was centrifuged at 12,000 ×*g* for 10 min at 4 °C. Protein concentrations were determined with a bicinchoninic acid assay kit (Pierce, Rockford, IL, USA). The extracts were fractionated by sodium dodecyl sulfate-polyacrylamide gel electrophoresis and transferred to a polyvinylidene difluoride membrane. The membranes were incubated with antibodies against IP_3R, MFN1, MFN2, DRP1, FIS1, or GADPH at 4 °C overnight (Abcam, Cambridge, UK). Then, the membranes were incubated with horseradish peroxidase-conjugated anti-mouse or anti-rabbit antibodies for 2 h. The blots were washed and developed with an enhanced chemiluminescent system (Amersham Biosciences, Uppsala, Sweden) according to the manufacturer's protocol.

Transmission Electron Microscopy (TEM) Analysis

Cerebral VSMCs were washed three times in 0.1 mmol/L phosphate buffered solution (PBS), followed by fixation in 1% osmium tetroxide at 4 °C for 3 h. The samples were washed three times in 0.1 mmol/L PBS again and gradually dehydrated in alcohol at different concentrations at 4 °C. After replacing the solution with propylene oxide and embedding using the SPI-Chem Embedding Kit (SPI, Chicago, IL, USA), the samples were fixed at 70 °C for 8 h. The sections (70 nm) were prepared with a Leica EM UC6 ultramicrotome (Leica Microsystems, Wetzlar, Germany), placed on EM grids, and stained with 3% uranyl acetate-lead citrate solution (SPI), followed by washing, drying, and imaging using a JEM1230 TEM (JEOL, Tokyo, Japan).

Immunohistochemistry

Paraffin-embedded sections (3 μm) of the basilar arteries were mounted on Thermo Scientific SuperFrost™ plus slides and dried overnight. Briefly, the arterial sections were incubated with primary IP_3R antibody (Abcam). After washing with PBS, the horseradish peroxidase was developed with 3,3-diaminobenzadine (Roche Diagnostics, Mannheim, Germany) as the chromogen substrate. The sections were rinsed, dehydrated in ethanol, cleared in xylene, and mounted. IP_3R staining in the cerebrovascular sections was observed under a microscope.

Cytoplasmic, Mitochondrial, and SR Ca^{2+} Assay

Cytoplasmic, mitochondrial, and SR Ca^{2+} concentrations were determined using a flow cytometry system with the Ca^{2+} indicators Fluo-4 AM, X-Rhod-1 AM, and Fluo-5N, respectively. Isolated cerebral VSMCs were placed in Hank's balanced salt solution (Sigma-Aldrich, St. Louis, MO, USA) and incubated with Fluo-4 AM (5 μmmol/L), X-Rhod-1 AM (5 μmmol/L), and Fluo-5N (10 μmmol/L) for 60 min at 37 °C. The Ca^{2+} content in individual groups of VSMCs was analyzed with the BD LSRFortessa™ flow cytometer (BD Biosciences, Franklin Lakes, NJ, USA).

Measurement of K_V and BK_{Ca} Currents

The patch-clamp technique and whole-cell patch-clamp recordings were used to analyze the K_V and BK_{Ca} currents. Extracellular fluid (150 mmol/L choline chloride, 5 mmol/L KCl, 2 mmol/L $CaCl_2$, 1 mmol/L $MgCl_2$, 10 mmol/L HEPES, 1 mmol/L $CdCl_2$, and 10 mmol/L D-glucose; adjusted to pH 7.4 with KOH; 320 mOsm) was continuously perfused at a rate of 0.2 mL/min. The tip of the patch-clamp electrode was about 1–2 μm, and resistance was 6–10 MΩ. The internal fluid in the glass electrode was 120 mmol/L potassium gluconate, 20 mmol/L KCl, 2 mmol/L $MgCl_2$, 10 mmol/L EGTA, 10 mmol/L HEPES, 5 mmol/L Na_2 ATP, and 1 mmol/L $CaCl_2$; adjusted to pH 7.2 with KOH; osmotic pressure 320 mOsm). The clamping voltage was set to −80 mV, depolarization voltage was in steps of 10 mV from −70 mV to 70 mV (pulse duration of 400 ms), and whole-cell K_V current was recorded every 2s. The signals were processed and recorded with an EPC-10 amplifier (HEKA Elektronik, Lambrecht, Germany). To separate the BK_{Ca} and K_V currents from the total current, the BK_{Ca} channel inhibitors TEA (1 mmol/L) and CTX (100 nmol/L) were added to the extracellular fluid. The current densities and open probabilities of BK_{Ca} and K_V were calculated.

Measurement of Cerebrovascular Contraction

Cerebral vascular reactivity was measured as described previously[25]. Briefly, basilar arteries (2 mm long) were carefully dissected free from the brain and mounted on two 40 μm stainless wires in the jaws of the Dual Wire Myograph System (Danish Myo Technology A/S, Hinnerup, Denmark) to record changes in isometric force. After the arteries were mounted and prepared, they were challenged with KCl (10–100 mmol/L) or cumulative concentrations (10^{-9}–10^{-5} mol/L) of 5-hydroxytryptamine (5-HT). Cumulative concentration response curves were generated.

Statistical Analysis

The results are expressed as mean ± standard error. GraphPad Prism 5.0 software (GraphPad Software Inc., La Jolla, CA, USA) was used for the statistical analysis. Protein expression and mRNA levels were compared using two-way analysis of variance (ANOVA) followed by the unpaired Student's *t*-test. The isometric force measurement data were analyzed by two-way ANOVA. A *P*-value of < 0.05 was considered significant.

RESULTS

General Data

Microgravity simulated by HU resulted in a significantly lower soleus muscle mass ($P < 0.001$). Soleus muscle-to-body mass ratios decreased significantly ($P < 0.001$) in the HU and HU + MT rats, which confirmed the efficacy of simulated microgravity by HU. The data are summarized in Table 1.

The Effects of HU on Ca^{2+} Distribution in VSMCs

Cytoplasmic, mitochondrial, and SR Ca^{2+} distribution and content in cerebral VSMCs are shown in Figure 1. After HU, cytoplasmic Ca^{2+} content significantly increased ($P < 0.001$) (Figure 1A, 1D) with a significant decrease of Ca^{2+} in mitochondria (Figure 1B, 1E) and the SR (Figure 1C, 1F) ($P < 0.001$) compared with CON rat cerebral VSMCs. The chronic treatment with mitoTEMPO restored cytoplasmic ($P < 0.001$), mitochondrial ($P < 0.01$), and SR ($P < 0.001$) Ca^{2+} distribution and content in HU + MT rat cerebral VSMCs.

Effects of HU on Mitochondrial Fission and Fusion

We analyzed mitochondrial fusion and fission to investigate the mechanism of cytoplasmic, mitochondrial, and SR Ca^{2+} redistribution (Figure 2). TEM (Figure 2A) showed more long and narrow mitochondria in the HU rat cerebral VSMCs, while more elliptical mitochondria were observed in the CON, CON + MT, and HU + MT rat cerebral VSMCs (mitochondria are marked by white arrows), indicating that HU enhanced mitochondrial fission and that treatment with mitoTEMPO attenuates mitochondrial fission. The MFN1/2 protein and mRNA levels (Figure 2B, 2F and Figure 2C, 2G) in HU rat cerebral VSMCs decreased significantly compared to those in the CON rats ($P < 0.001$). The DRP1/FIS1 protein and mRNA levels (Figure 2D, 2H and Figure 2E, 2I) were significantly higher in HU rat cerebral arteries than those in the CON rats ($P < 0.01$ for protein and $P < 0.001$ for mRNA). Chronic treatment with mitoTEMPO significantly upregulated the expression of MFN1/2 ($P < 0.05$ for MFN1 mRNA; $P < 0.001$ for MFN1/2 protein and MFN2 mRNA) but decreased the expression of FIS1/DRP1 ($P < 0.01$ for protein and $P < 0.001$ for mRNA) compared to the HU.

Effects of HU on IP_3R Expression

To investigate whether cytoplasmic Ca^{2+} redistribution was IP_3R-dependent, we determined the abundance of the IP_3R in HU rat cerebral arteries (Figure 3). IP_3R protein ($P < 0.001$) and mRNA ($P < 0.001$) levels increased significantly (Figure 3A and 3B) in HU rat cerebral arteries compared to the CON. Immunohistochemical staining revealed that the IP_3R was more positive in HU rat cerebral VSMCs than that in the CON (Figure 3C). Chronic treatment with mitoTEMPO partially restored the enhanced expression of the IP_3R after HU.

Effects of HU on Plasma Membrane Ion Channels

To investigate whether cytoplasmic Ca^{2+} redistribution induced by mitochondrial oxidative stress was associated with changes in plasma membrane K^+ channels, we analyzed total K^+ current,

Table 1. Body mass (g), soleus mass (mg), and soleus: body mass ratio (mg/g) of rats from the control, mitoTEMPO-treated control, hindlimb unweighting, and mitotempo-treated hindlimb unweighting groups (*n* = 8 in each group)

Group	Initial mass (g)	Final mass (g)	Soleus mass (mg)	Soleus: body mass (mg/g)
CON	198.60 ± 1.45	345.85 ± 10.47	134.54 ± 3.62	0.39 ± 0.01
HU	196.73 ± 2.07	336.79 ± 10.74	65.28 ± 1.85***	0.19 ± 0.01***
CON + MT	199.55 ± 2.67	338.57 ± 8.17	138.48 ± 2.82	0.41 ± 0.01
HU + MT	199.87 ± 1.80	341.89 ± 11.26	74.29 ± 2.12***	0.22 ± 0.01***

Note. CON, control; HU, hindlimb unweighting; MT, mitoTEMPO; CON+MT, mitoTEMPO-treated control; HU + MT, mitoTEMPO-treated HU. Values are mean ± standard error. $^{***}P < 0.001$ *vs.* control.

current densities, and open probabilities (Po) of the K_V and BK_{Ca} channels (Figure 4). Total K^+ current decreased (Figure 4A), whereas current densities and open probabilities of K_V (Figure 4B and 4C) and BK_{Ca} (Figure 4D and 4E) decreased and increased, respectively, compared to control rats, in HU rat cerebral VSMCs, which were restored by chronic treatment with mitoTEMPO.

Effects of HU on Cerebrovascular Contraction

To investigate whether the changes in cytoplasmic Ca^{2+} were associated with cerebrovascular contraction, we studied the cerebrovascular contraction to vasoconstrictors (Figure 5). Cumulative increases in KCl and 5-HT concentrations induced concentration-dependent vasoconstriction in basilar arteries from the four groups. Three-week HU significantly enhanced the maximal contractile responses to KCl and 5-HT in rat basilar arteries (P < 0.05) compared to the CON, which was attenuated by the chronic mitoTEMPO treatment (P < 0.05).

DISCUSSION

The major findings of the present study are: (1)

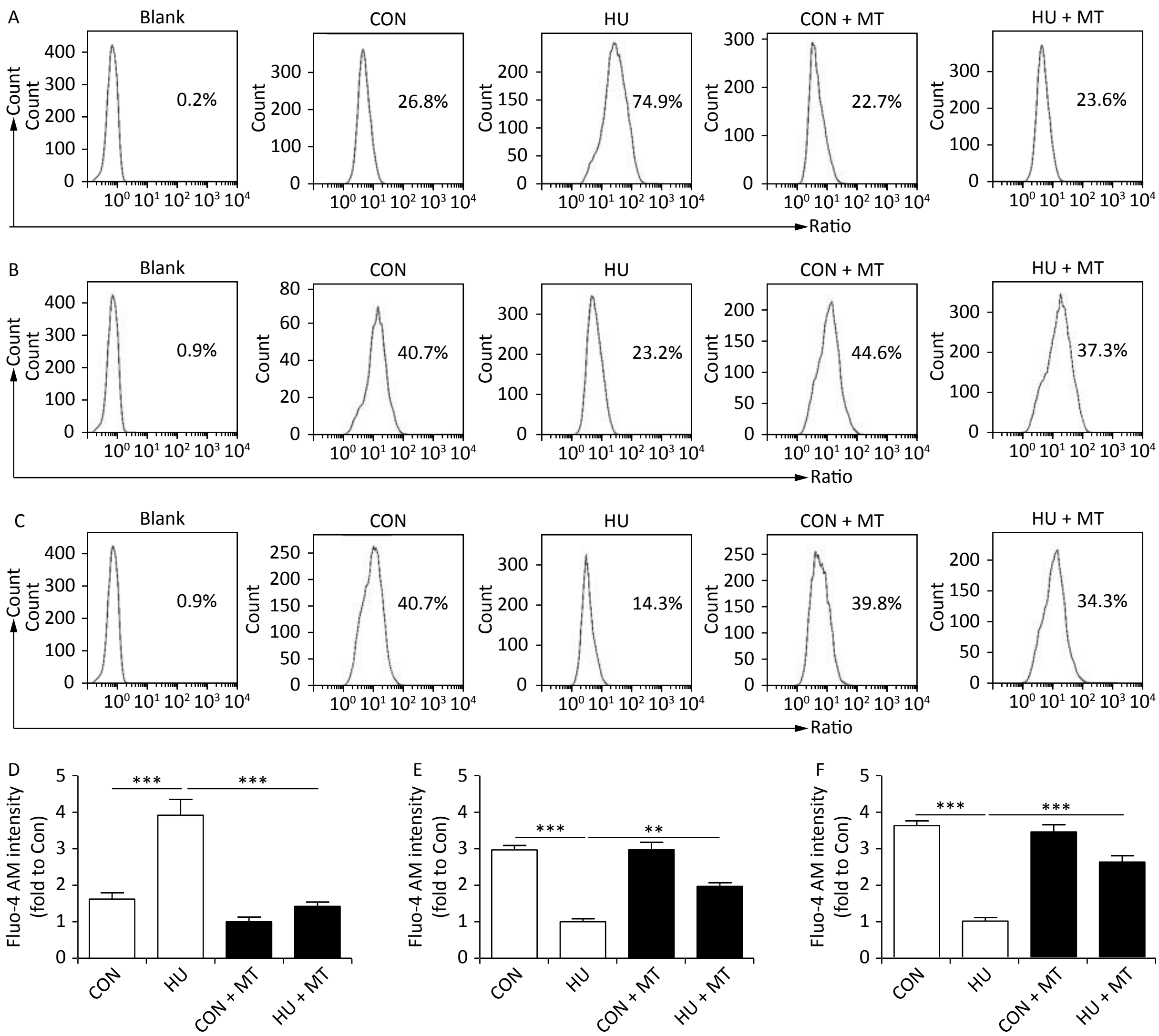

Figure 1. The effects of mitoTEMPO on cytoplasmic (A, D), mitochondrial (B, E), and sarcoplasmic reticulum (C, F) Ca^{2+} distribution in rat cerebral vascular smooth muscle cells. CON, control; HU, hindlimb unweighting; MT, mitoTEMPO; CON + MT, mitoTEMPO-treated control; HU + MT, mitoTEMPO-treated HU. Values are mean ± standard error. $^{**}P$ < 0.01 and $^{***}P$ < 0.001.

mitochondrial oxidative stress augmented HU rat cerebrovascular contraction to vasoconstrictors by regulating Ca^{2+} distribution and content in VSMCs; (2) mitochondrial oxidative stress regulated Ca^{2+} homeostasis by controlling IP_3R abundance, Ca^{2+} storage, mitochondrial fusion/fission, and changes in plasma membrane ion channels (K_V and BK_{Ca}) in HU rat cerebral VSMCs.

Exposure to microgravity results in postflight cardiovascular deconditioning and orthostatic intolerance in astronauts. Structural and functional remodeling of the cardiovascular system have been implicated in this process. We and other authors have found increased myogenic tone, enhanced vasoconstriction, and attenuated endothelium-dependent relaxation in HU rat cerebral

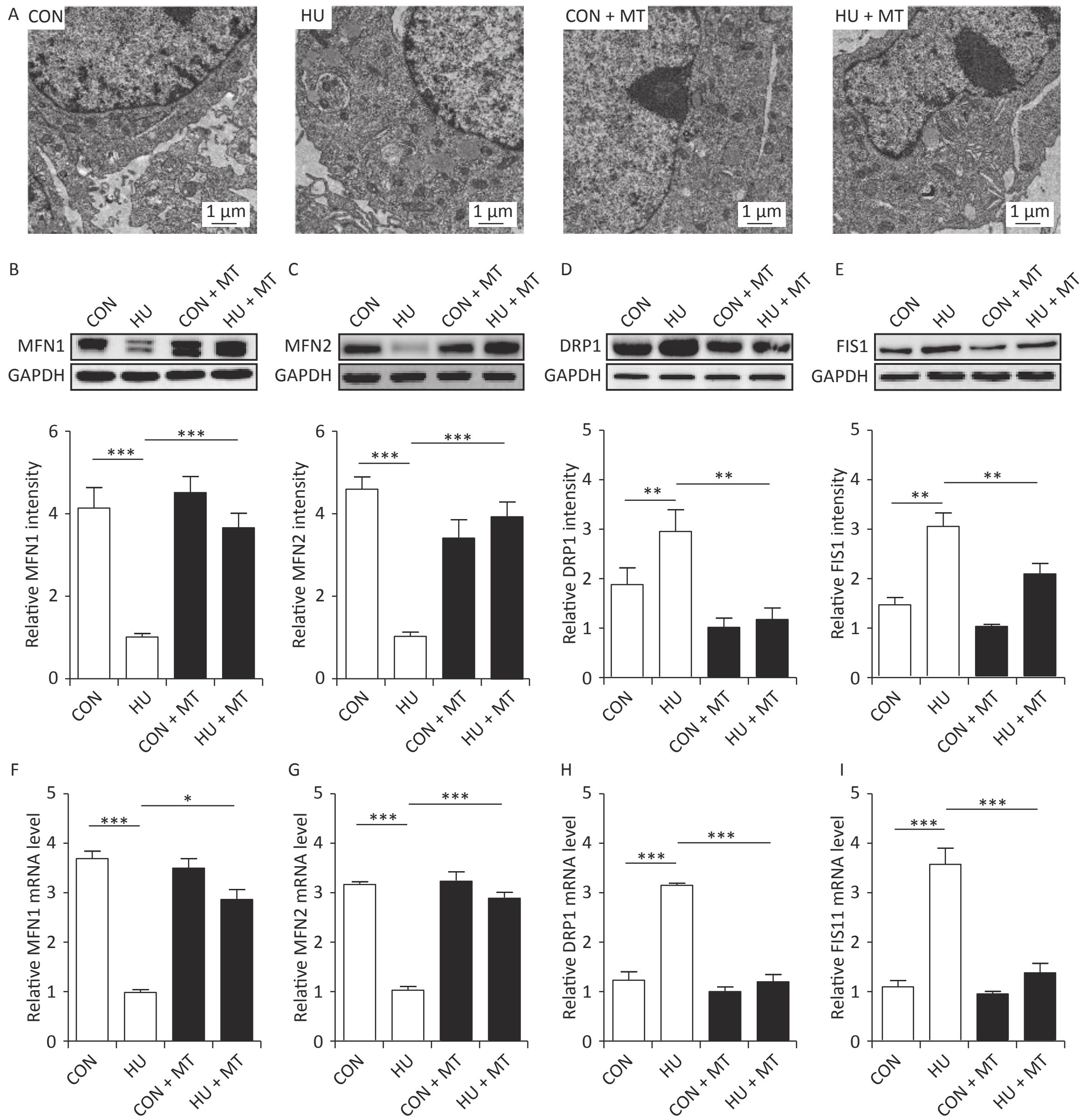

Figure 2. Effects of mitoTEMPO on mitochondrial fission and fusion (A) and the protein and mRNA levels of mitofusion 1 (MFN1) (B, F) and mitofusion 2 (MFN2) (C, G), dynamin-related protein 1 (DRP1) (D, H), and fission protein 1 (FIS1) (E, I) in rat cerebral vascular smooth muscle cells. CON, control; HU, hindlimb unweighting; MT, mitoTEMPO; CON + MT, mitoTEMPO-treated control; HU + MT, mitoTEMPO-treated HU. Values are mean ± standard error. $^{*}P$ < 0.05, $^{**}P$ < 0.01, and $^{***}P$ < 0.001.

arteries[3,4,6,25]. We previously reported mitochondrial oxidative stress and ER stress in rat cerebral VSMCs[21-23,26]. However, whether and how mitochondrial oxidative stress regulates HU rat

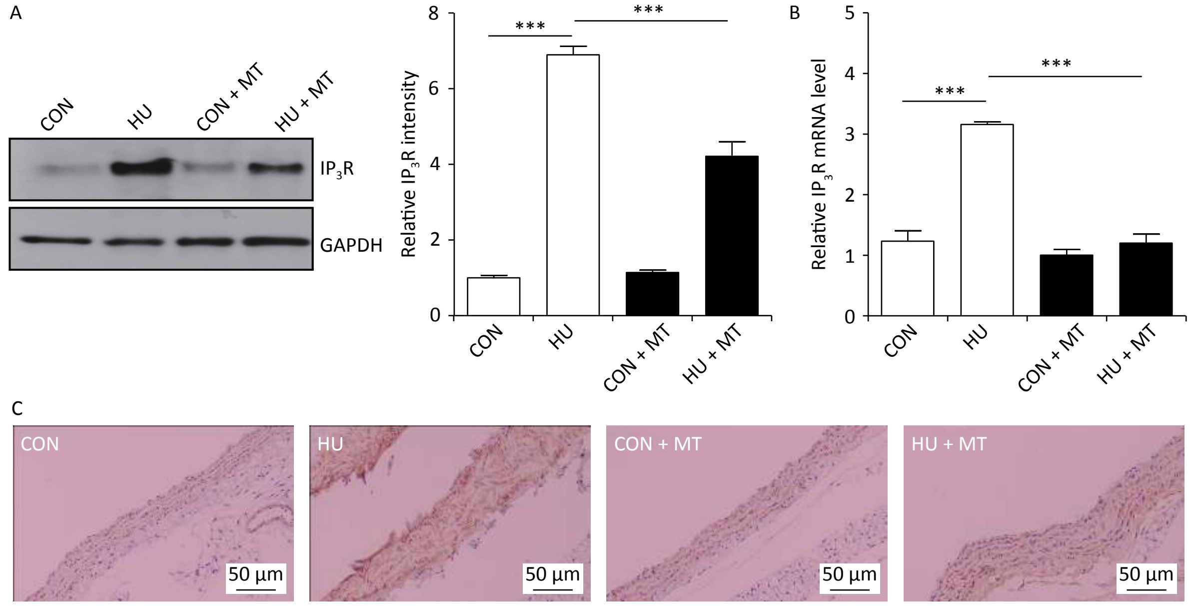

Figure 3. The effects of mitoTEMPO on protein (A) and mRNA (B) levels of the inositol 1,4,5-trisphosphate receptor (IP_3R) and immunohistochemistry for IP_3R (C) in rat cerebral vascular smooth muscle cells. CON, control; HU, hindlimb unweighting; MT, mitoTEMPO; CON + MT, mitoTEMPO-treated control; HU + MT, mitoTEMPO-treated HU. Values are mean ± standard error. $^{***}P < 0.001$.

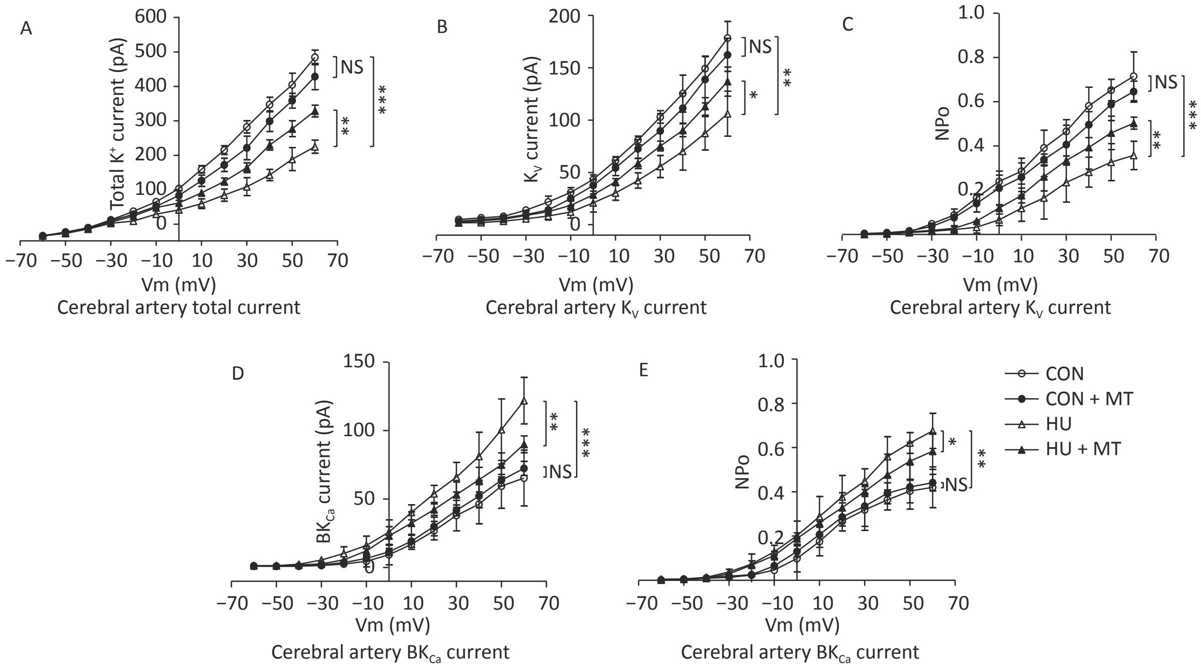

Figure 4. Effects of mitoTEMPO on total K^+ current (A), current activation, and opening probabilities of voltage-gated potassium (K_V) channels (B, C), and Ca^{2+}-activated K^+ (BK_{Ca}) channels (D, E) in rat cerebral vascular smooth muscle cells. CON, control; HU, hindlimb unweighting; MT, mitoTEMPO; CON + MT, mitoTEMPO-treated control; HU + MT, mitoTEMPO-treated HU. Values are mean ± standard error. $^{*}P < 0.05$, $^{**}P < 0.01$, and $^{***}P < 0.001$.

cerebrovascular reactivity remains unclear. The dynamic changes in cytoplasmic Ca^{2+} are a critical mechanism regulating vascular tone and contraction. During microgravity, large-conductance calcium-activated K^+ (BK_{Ca}) and L-type voltage-dependent Ca^{2+} (Ca_L) channels were activated in VSMCs, which are associated with apoptosis[10,11]. The Ca_L currents densities increased significantly in 4-week HU rat cerebral VSMCs, and therefore induced significantly higher cytoplasmic Ca^{2+} and enhanced vasoconstriction[27]. K_V channels are expressed in blood vessels and are key regulators of vascular tension. An increase in cytoplasmic Ca^{2+} concentration inactivates K_V channels and induces vascular contraction[28]. The BK_{Ca} channels in the vasculature located close to the IP_3Rs in the SR and the IP_3Rs stimulate the opening of BK_{Ca} channels dependent on Ca^{2+} released from IP_3Rs as in VSMCs[29]. In the current study, K_V and BK_{Ca} current densities and open probabilities, which are both important Ca^{2+}-regulating plasma ion channels, decreased and increased respectively; however, these changes were restored by the mitochondrial-targeted antioxidant mitoTEMPO. This means that mitochondrial oxidative stress regulates cytoplasmic Ca^{2+} concentration through the activities of plasma ion channels, which play roles in Ca^{2+} homeostasis in VSMCs exposed to microgravity or simulated microgravity.

The processes influencing cytoplasmic Ca^{2+} are important regulators of vascular function under physiological and pathophysiological settings. The mitochondria and SR are the major Ca^{2+} stores in VSMCs, which regulate Ca^{2+} homeostasis in intracellular organelles by Ca^{2+} sequestering activities[13]. The close connection between mitochondria and the SR plays an important role in mitochondrial dynamics, ATP production, lipid synthesis, and Ca^{2+} signaling[30,31]. Mitochondria regulate intracellular Ca^{2+} content through Ca^{2+} uptake from SR *via* the SR-mitochondrial membrane[32]. The rate of mitochondrial Ca^{2+} uptake is affected by the IP_3R and MFN2[33,34], which maintain the balance between extracellular and intracellular $[Ca^{2+}]$[13]. The IP_3R is a pivotal Ca^{2+} release channel located perinuclearly and peripherally in the SR[35]. ER/SR stress facilitates Ca^{2+} release from the SR through the IP_3R[14], which causes Ca^{2+} uptake by mitochondria. Increased mitochondrial Ca^{2+} influx leads to mitochondrial Ca^{2+} overload and opening of the mitochondrial permeability transition pore, eventually triggering cell death[36,37]. Overloading of Ca^{2+} within the mitochondrial matrix inhibits ATP production but promotes mitochondrial ROS production[38,39]. In the current study, increased IP_3R protein abundance and decreased SR Ca^{2+} in HU rat cerebral VSMCs suggested that IP_3R-dependent Ca^{2+} release from the SR was activated and increased cytoplasmic Ca^{2+} contributed to enhance vasoconstriction.

The elevated ROS levels in mitochondria and the SR send feedback for SR membrane Ca^{2+} release by stimulating the IP_3R[40,41], and increased ROS production enhances the rate of mitochondrial Ca^{2+} uptake and has a destructive effect on mitochondria, leading to changes in the state of mitochondria from fusion to fission by inducing the expression of DRP1 and FIS1[19,42]. Mitochondrial fusion provides the proper environment for Ca^{2+} regulation and cellular metabolism, which is important for Ca^{2+} homeostasis in VSMCs[19,43]. MFN1 and MFN2 play critical roles maintaining the correct mitochondrial and the SR-mitochondria connection, respectively[33,44]. MFN2,

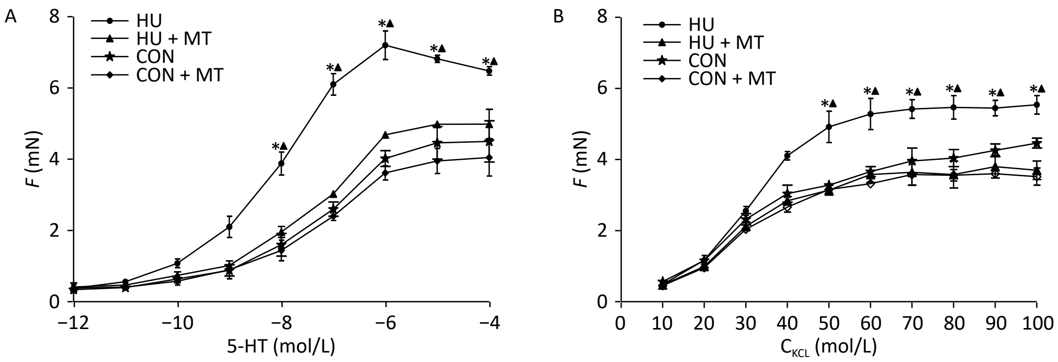

Figure 5. Effects of mitoTEMPO on vasoconstriction to cumulative KCl or 5-hydroxytryptamine (5-HT) in rat basilar arteries. CON, control; HU, hindlimb unweighting; MT, mitoTEMPO; CON + MT, mitoTEMPO-treated control; HU + MT, mitoTEMPO-treated HU. Values are mean ± standard error. $^*P < 0.05$ for HU *vs.* CON, $^▲P < 0.05$ for HU *vs.* HU + MT.

which is located in the outer mitochondrial membrane and SR membrane, tethers the SR to mitochondria and mediates Ca^{2+} signal transfer between the two organelles together with the IP_3R[45]. Once the mitochondrial dynamics have shifted from fusion to fission, cell death occurred caused by over-expression of FIS1, which depends on SR-mitochondria; Ca^{2+} signal transfer[46] and DRP1-induced mitochondrial fragmentation[47]. The Ca^{2+} redistribution leads to increased cytoplasmic Ca^{2+} and an enhanced contractile response to vasoconstrictors. Consistent with these findings, our present study showed that microgravity simulated by HU changed the morphological characteristics of the mitochondria from elliptical to long and narrow, along with upregulated expression of the mitochondrial fission proteins (DRP1 and FIS1) and decreased levels of the fusion proteins (MFN1 and MFN2), which were reversed by a mitochondrial-targeted antioxidant. This finding suggests that mitochondrial oxidative stress during simulated microgravity shifted the mitochondrial state from fusion to fission. Together with our previous findings that microgravity simulated by HU is associated with oxidative stress and mitochondrial oxidative stress in cerebral VSMCs[21,22,48], we infer that Ca^{2+} and ROS overloading in mitochondria during simulated microgravity leads to mitochondrial fission by regulating the expression of mitochondrial fission and fusion proteins. Therefore, mitochondrial oxidative stress induced by 3-weeks of HU stimulated Ca^{2+} release from the SR by upregulating IP_3R expression, impairing mitochondrial Ca^{2+} uptake, and undergoing mitochondrial fission, which resulted in the accumulation of Ca^{2+} in the cytoplasm and enhanced vasoconstriction.

Interestingly, our recent study reported that ER stress induces activation of the iNOS/NO-NF-κB/IκB pathway and plays a key role inducing endothelial inflammation and apoptosis[49]. Whether SR stress affects calcium signaling in cerebral VSMCs during microgravity simulation needs further investigation. Although we clarified that changes in calcium homeostasis caused by mitochondrial oxidative stress contributed to enhance vasoconstriction during simulated microgravity, we did not investigate the effects of mitochondrial oxidative stress on SR function. Further studies are needed to investigate functional alterations and the underlying mechanism of mitochondria and the SR during microgravity.

In conclusion, mitochondrial oxidative stress induced by simulated microgravity increased cytoplasmic Ca^{2+} by impairing mitochondrial fusion/fission-dependent Ca^{2+} uptake, enhancing IP_3R-dependent SR Ca^{2+} release, and regulating the functions of plasma K_V and BK_{Ca} channels. A mitochondrial-targeted antioxidant that alleviated mitochondrial oxidative stress restored Ca^{2+} homeostasis and vascular contraction to the agonists. The current results demonstrate that mitochondrial oxidative stress contributes to vasoconstriction by regulating calcium homeostasis in rat cerebrovascular smooth muscle cells exposed to simulated microgravity.

AUTHORS' CONTRIBUTIONS

Guarantor of integrity of the entire study: LIU Zi Fan. Study concept and design: ZHANG Ran and LI Xin. Experimental studies: LIU Zi Fan, WANG Hai Ming, JIANG Min, WANG Lin, XIE Man Jiang, LIN Le Jian, ZHAO Yun Zhang, SHAO Jun Jie, and ZHOU Jing Jing. Data analysis: LIU Zi Fan, WANG Hai Ming, and ZHANG Ran. Manuscript preparation: LIU Zi Fan and WANG Hai Ming. Manuscript editing: LIU Zi Fan and WANG Hai Ming. Manuscript review: ZHANG Ran and LI Xin. All authors have read and approved the final version of the manuscript.

CONFLICTS OF INTEREST

The authors declare no competing financial interests.

Received: August 19, 2020;
Accepted: October 20, 2020

REFERENCES

1. Convertino VA. Mechanisms of microgravity induced orthostatic intolerance: implications for effective countermeasures. J Gravit Physiol, 2002; 9, 1−13.
2. Hargens AR, Watenpaugh DE. Cardiovascular adaptation to spaceflight. Med Sci Sports Exerc, 1996; 28, 977−82.
3. Zhang LF. Vascular adaptation to microgravity: what have we learned? J Appl Physiol, 2001; 91, 2415−30.
4. Zhang LF. Region-specific vascular remodeling and its prevention by artificial gravity in weightless environment. Eur J Appl Physiol, 2013; 113, 2873−95.
5. Maier JAM, Cialdai F, Monici M, et al. The impact of microgravity and hypergravity on endothelial cells. BioMed Res Int, 2015; 2015, 434803.
6. Zhang R, Bai YG, Lin LJ, et al. Blockade of AT_1 receptor partially restores vasoreactivity, NOS expression, and superoxide levels in cerebral and carotid arteries of hindlimb unweighting rats. J Appl Physiol, 2009; 106, 251−8.
7. Zhang R, Ran HH, Ma J, et al. NAD(P)H oxidase inhibiting with apocynin improved vascular reactivity in tail-suspended hindlimb unweighting rat. J Physiol Biochem, 2012; 68, 99−105.
8. Shi F, Wang YC, Zhao TZ, et al. Effects of simulated

microgravity on human umbilical vein endothelial cell angiogenesis and role of the PI3K-Akt-eNOS signal pathway. PLoS One, 2012; 7, e40365.
9. Versari S, Villa A, Bradamante S, et al. Alterations of the actin cytoskeleton and increased nitric oxide synthesis are common features in human primary endothelial cell response to changes in gravity. Biochim Biophys Acta, 2007; 1773, 1645−52.
10. Xie MJ, Ma YG, Gao F, et al. Activation of BKCa channel is associated with increased apoptosis of cerebrovascular smooth muscle cells in simulated microgravity rats. Am J Physiol Cell Physiol, 2010; 298, C1489−500.
11. Xue JH, Zhang LF, Ma J, et al. Differential regulation of L-type Ca^{2+} channels in cerebral and mesenteric arteries after simulated microgravity in rats and its intervention by standing. Am J Physiol Heart Circ Physiol, 2007; 293, H691−701.
12. Islam MS. Calcium signaling: from basic to bedside. In: Islam M. Calcium Signaling. Springer. 2020, 1-6.
13. Liu ZW, Khalil RA. Evolving mechanisms of vascular smooth muscle contraction highlight key targets in vascular disease. Biochem Pharmacol, 2018; 153, 91−122.
14. Cioffi DL. Redox regulation of endothelial canonical transient receptor potential channels. Antioxid Redox Signal, 2011; 15, 1567−82.
15. Görlach A, Bertram K, Hudecova S, et al. Calcium and ROS: a mutual interplay. Redox Biol, 2015; 6, 260−71.
16. Zhang X, Yan SM, Zheng HL, et al. A mechanism underlying hypertensive occurrence in the metabolic syndrome: cooperative effect of oxidative stress and calcium accumulation in vascular smooth muscle cells. Horm Metab Res, 2014; 46, 126−32.
17. Hall AR, Burke N, Dongworth RK, et al. Mitochondrial fusion and fission proteins: novel therapeutic targets for combating cardiovascular disease. Br J Pharmacol, 2014; 171, 1890−906.
18. Wu SN, Lu QL, Wang QL, et al. Binding of FUN14 domain containing 1 with inositol 1, 4, 5-trisphosphate receptor in mitochondria-associated endoplasmic reticulum membranes maintains mitochondrial dynamics and function in hearts in Vivo. Circulation, 2017; 136, 2248−66.
19. Youle RJ, Van Der Bliek AM. Mitochondrial fission, fusion, and stress. Science, 2012; 337, 1062−5.
20. Yu R, Jin SB, Lendahl U, et al. Human Fis1 regulates mitochondrial dynamics through inhibition of the fusion machinery. EMBO J, 2019; 38, e99748.
21. Zhang R, Ran HH, Cai LL, et al. Simulated microgravity-induced mitochondrial dysfunction in rat cerebral arteries. FASEB J, 2014; 28, 2715−24.
22. Zhang R, Ran HH, Peng L, et al. Mitochondrial regulation of NADPH oxidase in hindlimb unweighting rat cerebral arteries. PLoS One, 2014; 9, e95916.
23. Peng L, Ran HH, Zhang Y, et al. NADPH oxidase accounts for changes in cerebrovascular redox status in hindlimb unweighting rats. Biomed Environ Sci, 2015; 28, 799−807.
24. Ren XL, Zhang R, Zhang YY, et al. Nitric oxide synthase activity in the abdominal aorta of rats is decreased after 4 weeks of simulated microgravity. Clin Exp Pharmacol Physiol, 2011; 38, 683−7.
25. Zhang R, Jia GL, Bao JX, et al. Increased vascular cell adhesion molecule-1 was associated with impaired endothelium-dependent relaxation of cerebral and carotid arteries in simulated microgravity rats. J Physiol Sci, 2008; 58, 67−73.
26. Zhang R, Jiang M, Zhang JB, et al. Regulation of the cerebrovascular smooth muscle cell phenotype by mitochondrial oxidative injury and endoplasmic reticulum stress in simulated microgravity rats *via* the PERK-eIF2α-ATF4-CHOP pathway. Biochim Biophys Acta Mol Basis Dis, 2020; 1866, 165799.
27. Xue JH, Chen LH, Zhao HZ, et al. Differential regulation and recovery of intracellular Ca^{2+} in cerebral and small mesenteric arterial smooth muscle cells of simulated microgravity rat. PLoS One, 2011; 6, e19775.
28. Shah VN, Chagot B, Chazin WJ. Calcium-dependent regulation of ion channels. Calcium Bind Proteins, 2006; 1, 203−12.
29. Cheng J, Wen J, Wang N, et al. Ion channels and vascular diseases. Arterioscler Thromb Vasc Biol, 2019; 39, e146−56.
30. Csordás G, Renken C, Várnai P, et al. Structural and functional features and significance of the physical linkage between ER and mitochondria. J Cell Biol, 2006; 174, 915−21.
31. Rowland AA, Voeltz GK. Endoplasmic reticulum-mitochondria contacts: function of the junction. Nat Rev Mol Cell Biol, 2012; 13, 607−25.
32. Sterea AM, El Hiani Y. The role of mitochondrial calcium signaling in the pathophysiology of cancer cells. In: Islam M. Calcium Signaling. Springer. 2020, 747-70.
33. De Brito OM, Scorrano L. Mitofusin 2 tethers endoplasmic reticulum to mitochondria. Nature, 2008; 456, 605−10.
34. Chernorudskiy AL, Zito E. Regulation of calcium homeostasis by ER redox: a close-up of the er/mitochondria connection. J Mol Biol, 2017; 429, 620−32.
35. Eid AH, El-Yazbi AF, Zouein F, et al. Inositol 1, 4, 5-trisphosphate receptors in hypertension. Front Physiol, 2018; 9, 1018.
36. Finkel T, Menazza S, Holmstrom KM, et al. The ins and outs of mitochondrial calcium. Circ Res, 2015; 116, 1810−9.
37. Vianello A, Casolo V, Petrussa E, et al. The mitochondrial permeability transition pore (PTP)-an example of multiple molecular exaptation? Biochim Biophys Acta Bioenerg, 2012; 1817, 2072−86.
38. Feno S, Butera G, Reane DV, et al. Crosstalk between calcium and ROS in pathophysiological conditions. Oxid Med Cell Longev, 2019; 2019, 9324018.
39. Kozlov AV, Lancaster JR JR, Meszaros AT, et al. Mitochondria-meditated pathways of organ failure upon inflammation. Redox Biol, 2017; 13, 170−81.
40. Avila G, De La Rosa JA, Monsalvo-Villegas A, et al. Ca^{2+} channels mediate bidirectional signaling between sarcolemma and sarcoplasmic reticulum in muscle cells. Cells, 2019; 9, 55.
41. Bartok A, Weaver D, Golenár T, et al. IP3 receptor isoforms differently regulate ER-mitochondrial contacts and local calcium transfer. Nature Communications, 2019; 10, 3726.
42. Balaban RS, Nemoto S, Finkel T. Mitochondria, oxidants, and aging. Cell, 2005; 120, 483−95.
43. Archer SL. Mitochondrial dynamics-mitochondrial fission and fusion in human diseases. N Engl J Med, 2013; 369, 2236−51.
44. Cipolat S, De Brito OM, Dal Zilio B, et al. OPA1 requires mitofusin 1 to promote mitochondrial fusion. Proc Natl Acad Sci USA, 2004; 101, 15927−32.
45. Guerrero-Hernandez A, Sanchez-Vazquez VH, Martinez-Martinez E, et al. Sarco-endoplasmic reticulum calcium release model based on changes in the luminal calcium content. In: Islam M. Calcium Signaling. Springer. 2020, 337-70.
46. Alirol E, James D, Huber D, et al. The mitochondrial fission protein hFis1 requires the endoplasmic reticulum gateway to induce apoptosis. Mol Biol Cell, 2006; 17, 4593−605.
47. Vallese F, Barazzuol L, Maso L, et al. ER-mitochondria calcium transfer, organelle contacts and neurodegenerative diseases. In: Islam M. Calcium Signaling. Springer. 2020, 719-46.
48. Zhang R, Ran HH, Gao YL, et al. Differential vascular cell adhesion molecule-1 expression and superoxide production in simulated microgravity rat vasculature. EXCLI J, 2010; 9, 195−204.
49. Jiang M, Wang HM, Liu ZF, et al. Endoplasmic reticulum stress-dependent activation of iNOS/NO-NF-κB signaling and NLRP3 inflammasome contributes to endothelial inflammation and apoptosis associated with microgravity. FASEB J, 2020; 34, 10835−49.